

# Microfluidic chip with integrated microvalves based on temperature- and pH-responsive hydrogel thin films

M. Bäcker<sup>1,2†</sup>, M. Raue<sup>3†</sup>, S. Schusser<sup>1,2</sup>, C. Jeitner<sup>1</sup>, L. Breuer<sup>1</sup>, P. Wagner<sup>4</sup>, A. Poghossian<sup>1,2</sup>, A. Förster<sup>1</sup>, T. Mang<sup>3</sup>, and M. J. Schöning<sup>\*1,2</sup>

<sup>1</sup>Institute of Nano- and Biotechnologies (INB), Aachen University of Applied Sciences, 52428 Jülich, Germany

<sup>2</sup>Peter Grünberg Institute (PGI-8), Research Centre Jülich, 52425 Jülich, Germany

<sup>3</sup>Institute of Applied Polymer Chemistry (IAP), Aachen University of Applied Sciences, 52428 Jülich, Germany

<sup>4</sup>Institute for Materials Research, Hasselt University, 3590 Diepenbeek, Belgium

Received 20 October 2011, revised 30 November 2011, accepted 11 January 2012

Published online 6 April 2012

**Keywords** microfluidics, microvalve, photopolymerization, responsive hydrogels

\* Corresponding author: e-mail schoening@fh-aachen.de, Phone: +49-241-6009-53215, Fax: +49-241-6009-53235

† Both the authors contributed equally to this work.

Two types of microvalves based on temperature-responsive poly(*N*-isopropylacrylamide) (PNIPAAm) and pH-responsive poly(sodium acrylate) (PSA) hydrogel films have been developed and tested. The PNIPAAm and PSA hydrogel films were prepared by means of *in situ* photopolymerization directly inside the fluidic channel of a microfluidic chip fabricated by combining Si and SU-8 technologies. The swelling/shrinking properties and height changes of the PNIPAAm and PSA films inside the fluidic channel were studied at temperatures of

deionized water from 14 to 36 °C and different pH values (pH 3–12) of Titrisol buffer, respectively. Additionally, in separate experiments, the lower critical solution temperature (LCST) of the PNIPAAm hydrogel was investigated by means of a differential scanning calorimetry (DSC) and a surface plasmon resonance (SPR) method. Mass-flow measurements have shown the feasibility of the prepared hydrogel films to work as an on-chip integrated temperature- or pH-responsive microvalve capable to switch the flow channel on/off.

© 2012 WILEY-VCH Verlag GmbH & Co. KGaA, Weinheim

**1 Introduction** Advances in micro- and nanofabrication and miniaturized biochemical analysis have resulted in the development of ‘Lab-on-a-chip’ (LOC) devices, which represent high-sophisticated devices with multiple functionalities, like the injection of buffer or analyte solution in a fluidic channel, the switching of flow channels (on/off), the control and regulation of the flow rate and direction, an active flow sorting down different paths dependent on the chemical composition of the fluid, etc. [1, 2]. An ideal LOC should combine multiple fluidic components (fluidic microchannels, micropumps, microvalves, mixers, etc.) as well as different sensors and actuators on a single device chip. However, the technological realization of the above mentioned functionalities and fluidic components on the same chip is very complicated and cost-intensive. Therefore, most of existing LOCs either include some external not-integrated fluidic components or they exhibit only certain single functionalities necessary for the concrete application.

Stimuli-responsive hydrogels integrated with microfluidic structures for the active flow control at micro-scale have attracted considerable attention during the last years [3–5]. Hydrogels are cross-linked polymer structures that are capable of absorbing a large amount of water. Stimuli-responsive hydrogels are able to change their volume (swelling or shrinking) significantly (more than hundred-fold) in response to small alterations of external stimuli such as pH, ionic strength, temperature, electric field, light, etc. [3–6]. They combine multiple sensing and actuation functions in a single component, and regulate the flow by expanding or contracting to seal or open the channel [7–12]. In contrast to typical conventional microfluidic actuators (*e.g.*, electromagnetic, piezoelectric or thermopneumatic), stimuli-responsive hydrogels can be integrated as a microfluidic component (*e.g.*, microvalves, micropumps) without the need for an external energy supply and complex fabrication schemes [7–12]. Thus, an application of stimuli-responsive hydrogels could significantly reduce the

microfluidic system complexity, keeping at the same time their multiple functionalities. The response time, which is solely determined by the hydrogel swelling/de-swelling kinetics, is one of the most crucial parameters for a successful implementation of hydrogels for sensor and actuator applications. Because the hydrogel response is typically diffusion-driven, scaling to micro-dimensions usually enhances the response time [8, 11, 13]. Although this field is very young, already a number of research groups worldwide has shown examples of stimulus-responsive hydrogel sensors and actuators. These include, for example, hydrogel-based pH [14–17], CO<sub>2</sub> [13, 18] and glucose [19] sensors, a blood sampling system that uses a temperature-responsive hydrogel to obtain a blood sample from a patient [20], hydrogel-based fluidic components such as microvalves for the control of liquid flow through microchannels [9, 21–23], micropumps [24], as well as flow-sorting [25] and mixing [26] systems. Eddington and Beebe presented a hydrogel-based microdispensing device able to precisely deliver a given amount of fluid over a specified time [7]. In addition, a very small pH-responsive valve for drug dosing applications has been developed in Ref. [27]. These valves were used to regulate the amount of drug flowing out of a drug reservoir. Moreover, the German company Gesim GmbH has developed a microvalve that uses a temperature-responsive hydrogel, controlled by a microheater [28]. Detailed reviews of the use of stimuli-responsive hydrogels in microfluidic devices and for sensor applications can be found, *e.g.*, in Refs. [7, 8, 11–16]. Most of the hydrogel-based fluidic components reported so far concern stimuli-responsive materials responding to one stimulus, mostly, the pH value or temperature. A combination of two or more different kinds of responsive hydrogels in a microfluidic system could provide more functionalities for tuning the flow by the different external stimuli. Moreover, an integration of different kinds of responsive hydrogels, stimuli elements (*e.g.*, integrated heater [28] or H<sup>+</sup>-ion generator for a local pH change [29–33]) and control sensors (*e.g.*, temperature or conductivity sensor, Si-based pH sensor [34, 35]) on the same chip and their combination with logic principles might create a new generation of LOCs, where each hydrogel component could be addressably perform the sensing, actuating or regulating functions in accordance to a logic signal that is ‘programmed’ in the system.

In this work, we present results of investigation of two types of microvalves based on temperature-responsive poly(*N*-isopropylacrylamide) (PNIPAAm) and pH-responsive poly(sodium acrylate) (PSA) hydrogel films prepared directly inside the flow channel of a microfluidic chip. The microfluidic chip has been fabricated by combining Si and SU-8 technologies. PNIPAAm is one of the most frequently used temperature-responsive hydrogels for fluidic applications (see *e.g.*, Refs. [8, 11, 24]), while PSA hydrogel films, to our knowledge, have not been applied for the development of on-chip integrated pH-responsive microvalves, so far. Temperature- and pH-sensitive hydrogels are very different in their physical behaviour and swelling mechanism. Since

the switching of hydrogel films is a crucial parameter that determines the microvalve design and performance, the swelling/shrinking properties of the patterned PNIPAAm and PSA films were directly studied inside the fluidic channel using the microscope of a contact-angle meter. Additionally, in separate experiments, the lower critical solution temperature (LCST) of the temperature-responsive PNIPAAm hydrogel was investigated by means of differential scanning calorimetry (DSC) and surface plasmon resonance (SPR) method.

## 2 Experimental

### 2.1 Materials

*N*-isopropylacrylamide (NIPAAm, 99%, Sigma–Aldrich), sodium acrylate (SA, 97%, Sigma–Aldrich), cross-linking agent *N,N'*-methylenebis(acrylamide) (BIS, 98%, Merck) and the photoinitiator Irgacure 2959 (Ciba) were of research grade and were used as received from commercial sources without any additional purification. The temperature- and pH-responsive hydrogels were prepared from a pre-polymer solution consisting of 100 mM monomer (NIPAAm or SA), 1 mM (for PNIPAAm) or 5 mM (for PSA) BIS and 0.45 mmol Irgacure dissolved in 60 mL deionized water under stirring. After dissolving the pre-polymer solution was degassed by argon for 30 min.

### 2.1.1 Design and fabrication of microfluidic chip

The microfluidic chip has been fabricated using Si and SU-8 technologies. The application of SU-8 photoresist with good qualities, like chemical resistance, high aspect ratio as well as mechanical and dielectric behaviour, is favoured for the fabrication of microcells and fluidic microchannels [36–38]. Figure 1 shows the schematic design of the microfluidic chip with the integrated microchannel and stimuli-responsive hydrogels for realizing the microvalve function. Additionally, the chip includes several single and meander-like thin-film metal electrodes, which could, in future experiments, serve as, *e.g.*, a local

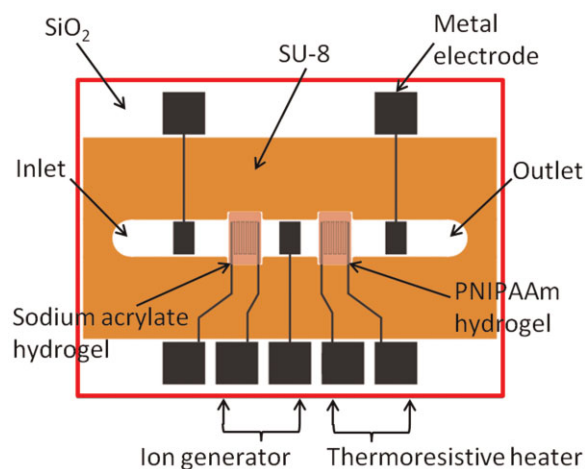


**Figure 1** (online colour at: [www.pss-a.com](http://www.pss-a.com)) Sketch of the microfluidic chip layout with integrated temperature- and pH-responsive hydrogel microvalves.

thermoresistive heater, an integrated temperature sensor or as H<sup>+</sup>-ion generator [29–34] for local pH changes via water electrolysis.

The technological steps of fabrication of the microfluidic chip can briefly be described as follows: first, 500 nm SiO<sub>2</sub> was grown by thermal wet oxidation of a p-Si wafer (Si-Mat) and partially etched to form trenches in the SiO<sub>2</sub> layer for buried metal electrodes. In the second step, the metal electrodes consisting of Ti (20 nm, as an adhesive layer)/Pt (200 nm) layers were deposited by means of electron-beam evaporation, patterned using the lift-off technique and then, passivated with a 5 μm SU-8 photoresist (Micro Resist Technology GmbH) layer. Afterwards, on top of this passivation layer, the flow channel itself was formed by structuring of a 100 μm thick SU-8 layer. The width of the channel was 1.75 mm having two broadenings of 2.5 mm for the hydrogel valves. Finally, the wafers were diced in chips with sizes of 15 mm × 20 mm. After the preparation of hydrogels inside the flow channel, the microfluidic chip was covered with a perspex coverplate having holes for inlet and outlet tubes and mounted on a printed circuit board (see Fig. 2).

**2.2 *In situ* preparation of hydrogel films** The PNIPAAm and PSA hydrogel films were prepared inside the fluidic channel by the *in situ* photopolymerization method [7, 39]. For this, the microfluidic channel was filled with the pre-polymer solution consisting of the respective monomers (NIPAAm or SA), cross-linking agent and photoinitiator (see Section 2.1). In order to improve the adhesion of the PSA hydrogel to the substrate, the silicon dioxide was silanized in a mixture of 10% γ-MPS (3-(trimethoxysilyl)propyl methacrylate (Sigma–Aldrich Co., St. Louis, USA) and toluene. The channel was topped with a coverslip to prevent drying of the monomer solution during the exposure and to ensure flatness of the solution (see Fig. 3).

Patterning of the monomer solution was performed using a mask aligner (MJB 3, Süss MicroTec) with a mercury lamp producing an irradiance of 10 mW/cm<sup>2</sup>. The pre-polymer solution was exposed to UV light (365 nm) through a photomask with a 1.5 mm × 2.45 mm hole, which defines the

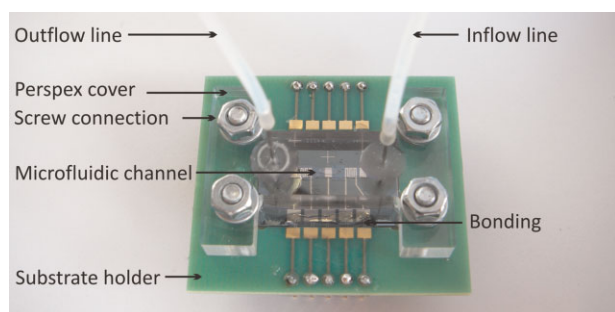


**Figure 2** (online colour at: www.pss-a.com) Assembled microfluidic chip with perspex cover and connection tubes.

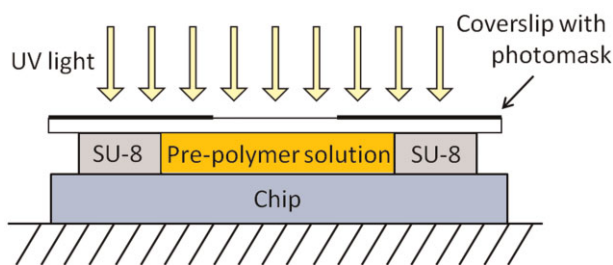


**Figure 3** (online colour at: www.pss-a.com) Schematic setup for *in situ* photopolymerization.

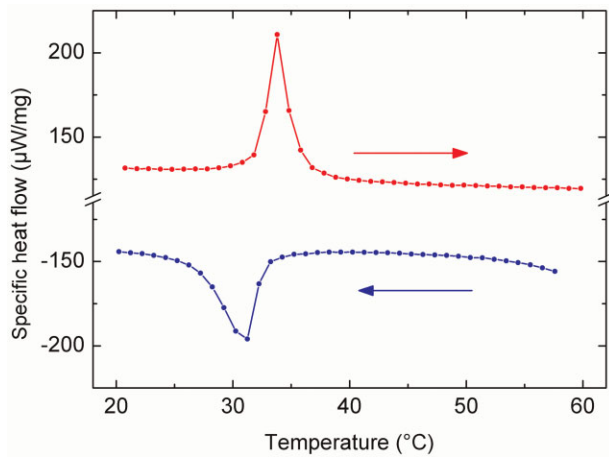
sizes of the hydrogel spots. Exposure time was 3 and 5 min for the PSA and PNIPAAm gels, respectively. Afterwards, the coverslip was carefully removed and the channel was rinsed to remove non-polymerized residues and then, hydrogels were left to dry at ambient temperature. The described method allows integration of multiple stimuli-responsive hydrogels of different shapes and sizes on the same microfluidic chip. The preparation of PNIPAAm hydrogels for the DSC and SPR measurements is described in Section 3.1.

### 3 Results and discussion

**3.1 Determination of LCST of PNIPAAm hydrogels by means of DSC and SPR methods** The PNIPAAm is one of the best known temperature-responsive hydrogels with a high degree of swelling and large volume change. Typically, temperature-responsive hydrogels go through a phase transition in response to an external temperature stimulus. The LCST is an important parameter for the characterization of the phase-transition behaviour of hydrogels. In this study, the LCST of bulk PNIPAAm and hydrogel films was determined from the DSC and SPR measurement, respectively.

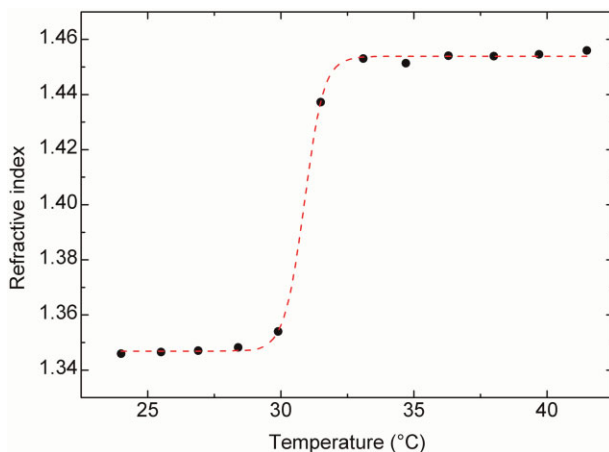
Temperature-sensitive hydrogels for the DSC measurements were prepared by the conventional photopolymerization method using UV light with a power of 0.04 mW/cm<sup>2</sup> for 12 h. Then, the samples were dried at 80 °C, crumpled, washed with deionized water and dried again. For the experiments, 15–30 mg of the partially swollen hydrogel film was placed into an aluminium pan and sealed with a lid. Afterwards, the sample was heated up from 4 to 60 °C and then, cooled to the starting temperature with a heating or cooling rate of 2 °C/min. This temperature program was repeated and the LCST of the PNIPAAm hydrogel was determined from the peaks in the DSC curve.

Figure 4 shows an example of the DSC curve of the prepared PNIPAAm hydrogel measured during heating and cooling cycles. At low temperatures the gel is in a highly swollen state. Above the phase-transition temperature, the polymer network chains collapse. The LCST of the prepared PNIPAAm hydrogels evaluated from the peaks in Fig. 4 is around 32–34 °C that is in good agreement with the results reported in literature [8, 40–42].



**Figure 4** (online colour at: [www.pss-a.com](http://www.pss-a.com)) DSC curve of the prepared PNIPAAm hydrogel measured during heating and cooling cycles.

In addition to DSC measurements, the SPR is a convenient method to study hydrogels in thin films and at interfaces [42–44]. The method is based on a measurement of the SPR angle shifts at different temperatures from which the refractive index of the hydrogel film can be evaluated as a function of temperature. For the SPR experiments, the hydrogel film was photopolymerized on top of an SPR slide (a gold-coated SF10 glass slide, Accurion GmbH, Germany). In accordance with well-known Kretschmann's configuration [44], the uncoated side was contacted to a prism made out of the same glass type. This stack was placed in a beam of an ellipsometric device (EP3, Accurion GmbH, Germany). The device features motor-controlled variation of the angle of incidence and a fluidic cell with build-in temperature control. During measurement, the fluidic system was set to a constant flow rate and filled with deionized water to provide constant conditions for all temperature states (collapsed,



**Figure 5** (online colour at: [www.pss-a.com](http://www.pss-a.com)) Refractive index of a PNIPAAm hydrogel film as a function of temperature evaluated from the SPR angle shifts.

swollen, intermediate). SPR measurements were performed at 811.2 nm wavelength at different temperature of the solution from 24 to 41.5 °C.

In Fig. 5 the temperature dependence of the refractive index of the PNIPAAm hydrogel film is presented. The high refractive index at high temperatures corresponds to a collapsed and hydrophobic gel phase containing little water, while the low refractive index at low temperatures corresponds to a swollen state with high water content. The refractive index is increased sharply above 30 °C. The refractive index reaches a steady state above and below the transition temperature with a transition region of about 1.5 °C. The inflection point of the curve at 31 °C can be defined as the phase-transition temperature. This value is something lower than evaluated from the DSC curve in Fig. 4, which can be attributed to different methods of measurements.

### 3.2 Characterization of hydrogel films with profilometry and microscopy

After photopolymerization, the dry hydrogel films were characterized by means of microscopy and profilometry. To minimize the effect of indentation on the measurement the stylus force of the profilometer was set to the lowest force possible. The optical micrographs of the patterned PNIPAAm and PSA gels in the SU-8 channel and the corresponding profilometer scans are presented in Figs. 6 and 7, respectively. The broadening in the SU-8 channel was almost completely filled by the hydrogel film. Both gels were relatively rough.

The sharp edges in the profilometer scan for the PSA hydrogel could be due to the removal of the coverslip after the photopolymerization. The average thickness of the hydrogel films in dry state was typically in the range of 8–10 µm.

For the characterization of the stimuli-responsive swelling behaviour of PNIPAAm and PSA hydrogel films directly inside the fluidic channel, the changes in the height (or thickness) of hydrogels in the channel induced by the respective stimulus (temperature or pH) have been investigated. For this, cross-sectional images of the PNIPAAm and PSA hydrogel films in the fluidic channel were taken at different temperatures of deionized water from 14 to 36 °C and different pH values of Titrisol buffer, respectively, using the microscope of a contact-angle meter (DataPhysics Instruments GmbH, Germany). From these cross-sectional images, the normalized height of the gel as function of temperature or pH value of the solution has been evaluated. The results of these experiments and schematic setups (inset graphs) are shown in Figs. 8 and 9.

At temperatures lower than the LCST, the PNIPAAm hydrogel is in a swollen state. As can be seen from Fig. 8, with increasing temperature the height of the PNIPAAm is reduced. The height of the hydrogel film at a starting temperature of 14 °C was taken as 100%. At room temperature the gel was still superior to the height of the channel walls. After raising the temperature above the LCST, morphological changes in terms of an increase of

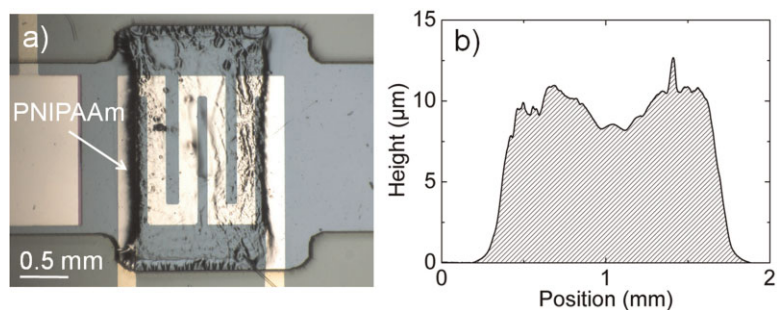


**Figure 6** (online colour at: [www.pss-a.com](http://www.pss-a.com)) Optical micrograph (a) and profilometer scan (b) of a dry PNIPAAm gel in the SU-8 channel.

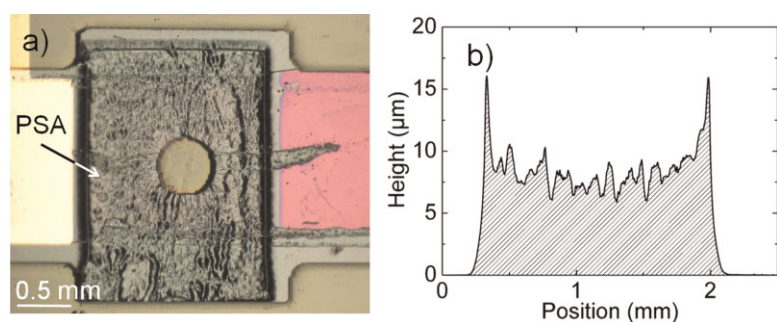


**Figure 7** (online colour at: [www.pss-a.com](http://www.pss-a.com)) Optical micrograph (a) and profilometer scan (b) of a dry PSA gel in the SU-8 channel.

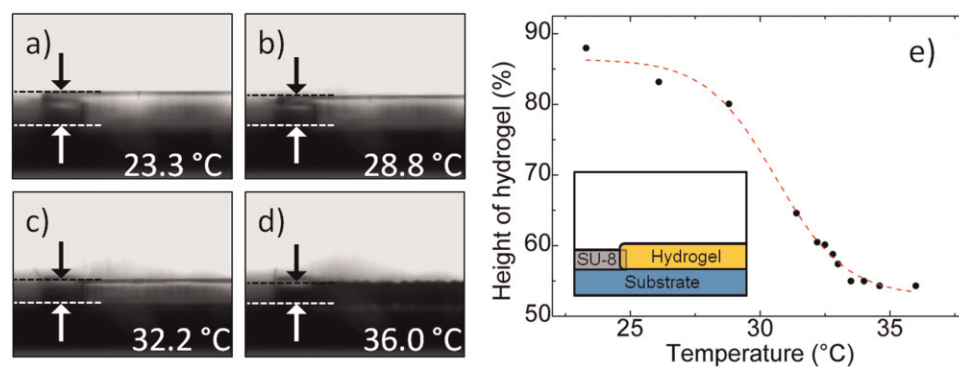


**Figure 8** (online colour at: [www.pss-a.com](http://www.pss-a.com)) Temperature-dependent swelling behaviour of the PNIPAAm hydrogel film inside the fluidic channel: (a–d) the cross-sectional images of the PNIPAAm films have been taken at different temperatures of 23.3, 28.8, 32.2 and 36 °C; (e) normalized height of the hydrogel as a function of temperature evaluated from the cross-sectional images. The height of the hydrogel at 14 °C was taken as 100%.

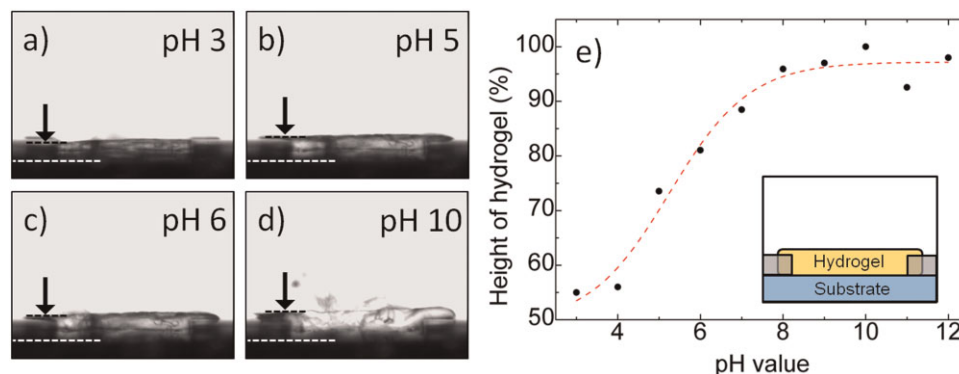


**Figure 9** (online colour at: [www.pss-a.com](http://www.pss-a.com)) pH-dependent swelling behaviour of the PSA hydrogel film inside the fluidic channel: (a–d) the cross-sectional images of the PSA films have been taken at pH 3, 5, 6 and 10; (e) normalized height of the hydrogel as a function of pH evaluated from the cross-sectional images. The height of the hydrogel at pH 10 was taken as 100%.

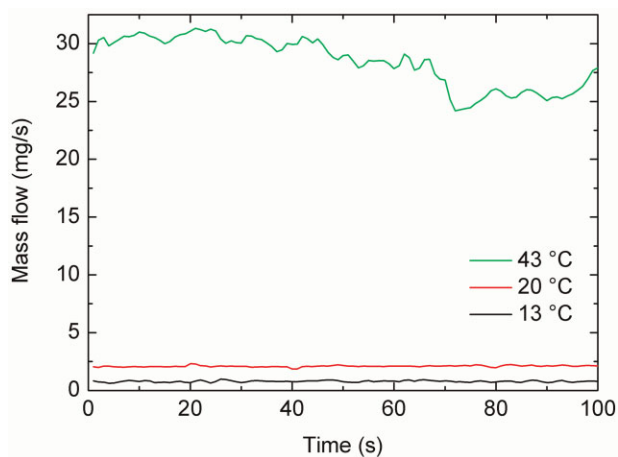


**Figure 10** (online colour at: [www.pss-a.com](http://www.pss-a.com)) Mass flow through the on-chip integrated PNIPAAm microvalve at different temperatures of 13, 20 and 43 °C.

waviness and an opaqueness of the gel were observed. The height of the hydrogel is sharply reduced at temperatures of 29–33 °C. The height of the hydrogel at 33 °C was about two times smaller than that of at 14 °C. No significant loss of height was observed in the temperature range of 34–36 °C. These results are in good agreement with the DSC measurements in Section 3.1.

The swelling behaviour of the pH-responsive PSA films inside the fluidic channel was investigated in Titrisol buffer solutions from pH 3 to 12. As an example, Fig. 9(a–d) shows the cross-sectional images of the PSA films taken at pH 3, 5, 6 and 10. The normalized height of the hydrogel as a function of pH evaluated from the cross-sectional images is shown in Fig. 9(e). Here, all values were scaled to the hydrogel height at pH 10. The steepest volume change was observed between pH 4 and 6. The overall height change in the range from pH 4 to 8 was approximately 40%. Further pH increase from pH 8 to 12 showed no considerable volume change.

### 3.3 On-chip integrated microvalve based on temperature- and pH-responsive hydrogels

To examine the feasibility of the prepared hydrogel films to work as an on-chip integrated microvalve capable to switch the flow channel ‘on/off’, mass-flow measurements were performed. For this, the inlet of the microfluidic channel was connected to a pump and the outlet to an electronic balance. Liquid was pumped into the channel and the mass flow at the outlet was recorded by the balance. The change of mass flow has been used to characterize the switching behaviour of the microvalve.

Figure 10 demonstrates the results of the mass-flow measurements through the on-chip integrated PNIPAAm microvalve at different chip temperatures of 13, 20 and 43 °C. In this experiment, the whole fluidic chip was immersed in a temperature-regulated water bath and deionized water was pumped into the inlet. As expected, at temperatures below the phase transition temperature, the

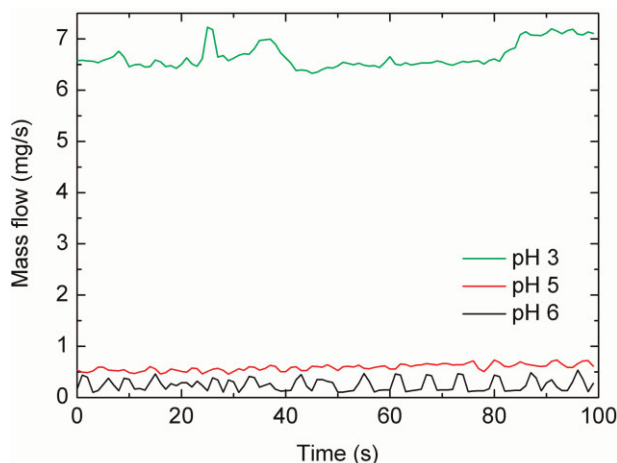


**Figure 11** (online colour at: [www.pss-a.com](http://www.pss-a.com)) Mass flow through the on-chip integrated PSA microvalve at different pH values of buffer solution.

PNIPAAm film behaved as a normally closed valve. The swollen hydrogel film blocks the fluidic channel, resulting in a mass flow of approximately 1 and 2 mg/s at 13 and 20 °C, respectively. As a result to the increase of temperature above the LCST, the PNIPAAm film collapsed, thereby decreasing the resistance of the fluid flow and allowing the fluid to flow through the channel. The observed mass flow at 43 °C was more than ten times higher than at room temperature.

Figure 11 demonstrates the results of the mass-flow measurements through the on-chip integrated pH-responsive PSA microvalve. In this experiment, Titrisol buffer solutions (Merck) with different pH values of pH 3, 5 and 6 were pumped into the fluidic channel. The highest mass flow was observed at pH 3, which is in good agreement with the results of the cross-sectional images in Fig. 9. With increasing the pH value of the buffer solution, a reduction of the mass flow was observed. The mass flow was almost completely suppressed at pH 6.

Typically, the mass flow through the PSA valve was overall lower than through the PNIPAAm valve. This could be attributed to the different filling degree of the fluidic channel with different hydrogels. Generally, the filling degree of the channel is one of the most important parameters of hydrogel-based fluidic components. Due to the softness of hydrogels, in principle, the fluidic channel can be filled completely with the swollen hydrogel, resulting in an ideal valve without any leakage flow. However, usually, hydrogel valves with a low filling level have a non-ideal behaviour and always show some leakage flow that has also been observed in our experiments with the temperature-responsive PNIPAAm hydrogels (see Fig. 10).

**4 Conclusions** In this work, two types of microvalves based on temperature-responsive PNIPAAm and pH-responsive PSA hydrogel films have been developed. The microfluidic chip has been fabricated by combining Si and

SU-8 technologies. The PNIPAAm and PSA hydrogel films were prepared inside the fluidic channel by *in situ* photopolymerization method. The LCST of temperature-responsive PNIPAAm hydrogels was investigated by means of the DSC and SPR methods. In addition, the swelling/deswelling behaviour and corresponding changes in the height of the patterned PNIPAAm and PSA films inside the fluidic channel have been studied using microscopy. Mass-flow measurements have shown the feasibility of the prepared hydrogel films to work as an on-chip integrated temperature- or pH-responsive microvalve capable to switch the flow channel on/off.

Future works will be directed to realize temperature- and pH-responsive microvalves, which could addressably be activated by means of on-chip integrated stimuli elements such as a thermoresistive heater or H<sup>+</sup>-ion generator-electrode for local pH changes via water electrolysis.

**Acknowledgements** Financial support of the Aachen University of Applied Sciences is gratefully acknowledged.

## References

- [1] D. Mark, S. Haeberle, G. Roth, F. von Stetten, and R. Zengerle, *Chem. Soc. Rev.* **39**, 1153 (2010).
- [2] M. L. Kovarik and S. C. Jacobson, *Anal. Chem.* **81**, 7133 (2009).
- [3] N. A. Peppas, J. Z. Hilt, A. Khademhosseini, and R. Langer, *Adv. Mater.* **18**, 1345 (2006).
- [4] I. Tokarev and S. Minko, *Soft Matter* **5**, 511 (2009).
- [5] C. de las Heras Alarcon, S. Pennadam, and C. Alexander, *Chem. Soc. Rev.* **34**, 276 (2005).
- [6] T. Khaleque, S. Abu-Salih, J. R. Saunders, and W. Moussa, *J. Nanosci. Nanotechnol.* **11**, 2470 (2011).
- [7] D. T. Eddington and D. J. Beebe, *Adv. Drug Delivery Rev.* **56**, 199 (2004).
- [8] K.-F. Arndt, D. Kuckling, and A. Richter, *Polym. Adv. Technol.* **11**, 496 (2000).
- [9] D. J. Beebe, J. S. Moore, J. M. Bauer, Q. Yu, R. H. Liu, C. Devadoss, and B.-H. Jo, *Nature* **404**, 588 (2000).
- [10] V. C. Ayala, M. Michalzik, S. Harling, H. Menzel, F. A. Guarnieri, and S. Büttgenbach, *J. Phys.: Conf. Ser.* **90**, 012025 (2007).
- [11] L. Dong and H. Jiang, *Soft Matter* **3**, 1223 (2007).
- [12] K. Deligkaris, T. S. Tadele, W. Olthuis, and A. van den Berg, *Sens. Actuators B* **147**, 765 (2010).
- [13] H. J. van der Linden, S. Herber, W. Olthuis, and P. Bergveld, *Analyst* **128**, 325 (2003).
- [14] A. Richter, G. Paschew, S. Klatt, J. Lienig, K.-F. Arndt, and H.-J. P. Adler, *Sensors* **8**, 561 (2008).
- [15] G. Gerlach, H. Guenther, G. Suchaneck, J. Sorber, K.-F. Arndt, and A. Richter, *Macromol. Symp.* **210**, 403 (2004).
- [16] G. Gerlach, M. Guenther, J. Sorber, G. Suchaneck, K.-F. Arndt, and A. Richter, *Sens. Actuators B* **111–112**, 555 (2005).
- [17] C. Ruan, K. G. Ong, C. Mungle, M. Paulose, N. J. Nickl, and C. A. Grimes, *Sens. Actuators B* **96**, 61 (2003).
- [18] S. Herber, J. Bomer, W. Olthuis, P. Bergveld, and A. van den Berg, *Biomed. Microdevices* **7**, 197 (2005).
- [19] M. Schwartz, H. Guterma, and J. Kost, *J. Biomed. Mater. Res.* **41**, 65 (1998).
- [20] K. Kobayashi and H. Suzuki, *Sens. Actuators B* **80**, 1 (2001).
- [21] J. Wang, Z. Chen, M. Mauk, K.-S. Hong, M. Li, S. Yang, and H. H. Bau, *Biomed. Microdevices* **7**, 313 (2005).
- [22] R. H. Liu, Q. Yu, and D. J. Beebe, *J. Microelectromech. Syst.* **11**, 45 (2001).
- [23] S. Rahimi, E. H. Sarraf, G. K. Wong, and K. Takahata, *Biomed. Microdevices* **13**, 267 (2011).
- [24] A. Richter, S. Klatt, G. Paschew, and C. Klenke, *Lab Chip* **9**, 613 (2009).
- [25] T. Arakawa, Y. Shirasaki, T. Aoki, T. Funatsu, and S. Shoji, *Sens. Actuators A* **135**, 99 (2007).
- [26] J. B. Prettyman and D. T. Eddington, *Sens. Actuators B* **157**, 722 (2011).
- [27] S. K. Deo, E. A. Moschou, S. F. Peteu, L. G. Bachas, S. Daunert, P. E. Eisenhardt, and M. J. Madou, *Anal. Chem.* **75**, 207A (2003).
- [28] www.gesim.de (2.4.2010).
- [29] A. Poghossian, L. Berndsen, and M. J. Schöning, *Sens. Actuators B* **95**, 384 (2003).
- [30] A. Poghossian, T. Yoshinobu, and M. J. Schöning, *Sensors* **3**, 202 (2003).
- [31] A. Poghossian, J. W. Schultze, and M. J. Schöning, *Sens. Actuators B* **91**, 83 (2003).
- [32] A. Poghossian, J. W. Schultze, and M. J. Schöning, *Electrochim. Acta* **48**, 3289 (2003).
- [33] A. Poghossian and M. J. Schöning, *Electroanalysis* **16**, 1863 (2004).
- [34] M. Bäcker, S. Beging, M. Biselli, A. Poghossian, J. Wang, W. Zang, P. Wagner, and M. J. Schöning, *Electrochim. Acta* **54**, 6107 (2009).
- [35] M. Bäcker, S. Pouyeshman, Th. Schnitzler, A. Poghossian, P. Wagner, M. Biselli, and M. J. Schöning, *Phys. Status Solidi A* **208**, 1364 (2011).
- [36] J. C. Ribeiro, G. Minas, P. Turmezei, R. F. Wolfenbittel, and J. H. Correia, *Sens. Actuators A* **123–124**, 77 (2005).
- [37] M. J. Schöning, N. Näther, V. Auger, A. Poghossian, and M. Koudelka-Hep, *Sens. Actuators B* **108**, 986 (2005).
- [38] N. Näther, D. Rolka, A. Poghossian, M. Koudelka-Hep, and M. J. Schöning, *Electrochim. Acta* **51**, 924 (2005).
- [39] D. Singh, D. Kuckling, V. Choudhary, H.-J. Adler, and V. Koul, *Polym. Adv. Technol.* **17**, 186 (2006).
- [40] D. Kuckling, M. E. Harmon, and C. W. Frank, *Macromolecules* **35**, 6377 (2002).
- [41] D. Kuckling, J. Hoffmann, M. Plötner, D. Ferse, K. Kretschmer, H.-J. P. Adler, K.-F. Arndt, and R. Reichelt, *Polymer* **44**, 4455 (2003).
- [42] M. E. Harmon, T. A. M. Jakob, W. Knoll, and C. W. Frank, *Macromolecules* **35**, 5999 (2002).
- [43] I. Hirata, M. Okazaki, and H. Iwata, *Polymer* **45**, 5569 (2004).
- [44] M. E. Harmon, M. Tang, and C. W. Frank, *Polymer* **44**, 4547 (2003).